University of Groningen

Hansenula polymorpha Vam7p is required for macropexophagy

Stevens, Patricia; Monastyrska, Iryna; Leão-Helder, Adriana N.; van der Klei, Ida; Veenhuis, Marten; Kiel, Jan; Monastyrska, [No Value]

Published in:
Default journal

DOI:
10.1016/j.femsyr.2005.02.009

IMPORTANT NOTE: You are advised to consult the publisher's version (publisher's PDF) if you wish to cite from it. Please check the document version below.

Document Version
Publisher's PDF, also known as Version of record

Publication date:
2005

Link to publication in University of Groningen/UMCG research database

Citation for published version (APA):
Stevens, P., Monastyrska, I., Leão-Helder, A. N., Klei, I. J. V. D., Veenhuis, M., Kiel, J. A. K. W., & Monastyrska, . N. V. (2005). Hansenula polymorpha Vam7p is required for macropexophagy. Default journal, 5(11), 985 - 997. DOI: 10.1016/j.femsyr.2005.02.009

Copyright
Other than for strictly personal use, it is not permitted to download or to forward/distribute the text or part of it without the consent of the author(s) and/or copyright holder(s), unless the work is under an open content license (like Creative Commons).

Take-down policy
If you believe that this document breaches copyright please contact us providing details, and we will remove access to the work immediately and investigate your claim.

Downloaded from the University of Groningen/UMCG research database (Pure): http://www.rug.nl/research/portal. For technical reasons the number of authors shown on this cover page is limited to 10 maximum.

Download date: 10-02-2018

ELSEVIER

FEMS Yeast Research 5 (2005) 985–997

FEMS Yeast Research

www.fems-microbiology.org

Hansenula polymorpha Vam7p is required for macropexophagy

Patricia Stevens [1,2], Iryna Monastyrska [1,3], Adriana N. Leão-Helder [4], Ida J. van der Klei, Marten Veenhuis, Jan A.K.W. Kiel *

Eukaryotic Microbiology, Groningen Biomolecular Sciences and Biotechnology Institute (GBB), University of Groningen, P.O. Box 14, 9751 AA Haren, The Netherlands

Received 17 January 2005; received in revised form 23 February 2005; accepted 24 February 2005

First published online 19 April 2005

Abstract

We have analyzed the functions of two vacuolar t-SNAREs, Vam3p and Vam7p, in peroxisome degradation in the methylotrophic yeast *Hansenula polymorpha*. A *Hp-vam7* mutant was strongly affected in peroxisome degradation by selective macropexophagy as well as non-selective microautophagy. Deletion of Hp-Vam3p function had only a minor effect on peroxisome degradation processes. Both proteins were located at the vacuolar membrane, with Hp-Vam7p also having a partially cytosolic location. Previously, in baker's yeast Vam3p and Vam7p have been demonstrated to be components of a t-SNARE complex essential for vacuole biogenesis. We speculate that the function of this complex in macropexophagy includes a role in membrane fusion processes between the outer membrane layer of sequestered peroxisomes and the vacuolar membrane. Our data suggest that Hp-Vam3p may be functionally redundant in peroxisome degradation. Remarkably, deletion of *Hp-VAM7* also significantly affected peroxisome biogenesis and resulted in organelles with multiple, membrane-enclosed compartments. These morphological defects became first visible in cells that were in the mid-exponential growth phase of cultivation on methanol, and were correlated with accumulation of electron-dense extensions that were connected to mitochondria.
© 2005 Federation of European Microbiological Societies. Published by Elsevier B.V. All rights reserved.

Keywords: Autophagy; Peroxisome; Pexophagy; Selective organelle degradation; SNARE; Yeast

1. Introduction

At present, three modes of peroxisome degradation have been characterized. These include (i) selective peroxisome degradation (macropexophagy), (ii) selective, bulk uptake of peroxisomes into the vacuole (micropexophagy), and (iii) non-selective uptake of peroxisomes by microautophagy (reviewed by [1,2]). Macropexophagy is a prominent feature in methylotrophic yeast species (e.g. *Hansenula polymorpha* and *Pichia pastoris*) following the repression of methanol metabolism or inactivation of organelle function. In contrast, micropexophagy is yet only observed in *P. pastoris* cells as a response of the cells to excess glucose conditions (for review see [2]). Non-selective autophagy involves turnover of portions of cytoplasm (including peroxisomes) by the vacuole, either following sequestration into an autophagosome (macroautophagy; reviewed by [3]) or after uptake via a pinocytosis-like mechanism (microautophagy). In *H. polymorpha*, only the latter process has

* Corresponding author. Tel.: +31 50 3632218; fax: +31 50 3632154.
E-mail address: j.a.k.w.kiel@rug.nl (J.A.K.W. Kiel).
[1] These authors contributed equally to this manuscript.
[2] Current address: Department of Microbial Ecology, Centre of Ecological and Evolutionary Studies, University of Groningen, Kerklaan 30, 9751 NN Haren, the Netherlands.
[3] Current address: Life Sciences Institute, University of Michigan, 210 Washtenaw Avenue, Ann Arbor, MI 48109-2216, USA.
[4] Current address: Department of Cell Biology and Genetics, Rio de Janeiro State University, Av. São Francisco Xavier, 524, Pavilhão Haroldo Lisboa da Cunha, 2nd floor 20550-013. Rio de Janeiro – RJ, Brazil.

1567-1356/$22.00 © 2005 Federation of European Microbiological Societies. Published by Elsevier B.V. All rights reserved.
doi:10.1016/j.femsyr.2005.02.009

been observed, which is initiated by nitrogen limitation [1,4]. Very recently, the non-selective nature of autophagy was challenged by the finding that certain cytosolic components may be specific cargo during these autophagic processes [5].

Macropexophagy has been a topic of research of our laboratory for several years, using the methylotrophic yeast *H. polymorpha* as model organism. Characteristic for this process is that upon induction of macropexophagy organelles are degraded individually and sequentially (reviewed by [6]). At present, our research has focused on the principles of tagging organelles for degradation and, in addition, on the origin of the membranes that sequester peroxisomes. Recent data indicate that in *H. polymorpha* the machineries of peroxisome biogenesis and selective peroxisome degradation converge at the peroxin Pex14p [7]. Also a second peroxin, Pex3p, essential for peroxisome membrane formation, plays a role in the onset of macropexophagy [8]. These data led us to hypothesize that the initiation of peroxisome sequestration may be regulated via the function of membrane-bound peroxins. At present, little is known on the origin of the membranes that sequester peroxisomes during macropexophagy. However, based on the similarity between the two processes, we recently have proposed [6] that the principles of membrane formation during macropexophagy are reminiscent of those of the cytoplasm-to-vacuole-targeting (Cvt) pathway that sorts specific proteins (Ape1p and Ams1p) to the vacuole in *Saccharomyces cerevisiae* (reviewed by [9]). Two key components of the Cvt pathway are Atg19p and Atg11p (for the new nomenclature see [10]) that specifically deliver the cargo molecules Ape1p and Ams1p to the sequestering machinery. This machinery involves the function of Atg8p, that can be conjugated to phosphatidylethanolamine, and the pre-autophagosomal structure, a large, presumptive membranous scaffold to which various proteins involved in autophagy and the Cvt pathway are recruited. Upon completion of sequestration, fusion of the sequestered compartment (designated Cvt vesicle) with the vacuole takes place, a process that requires the function of SNARE proteins.

In a recent screen for macropexophagy mutants of *H. polymorpha* we have isolated a mutant that appeared to be disrupted in the *VAM3* gene. In *S. cerevisiae* *VAM3* encodes a t-SNARE involved in vacuole biogenesis, autophagy and the Cvt pathway [11,12], and is present in a *cis*-SNARE protein complex together with Vam7p [13,14]. This led us to isolate both the *H. polymorpha* *VAM3* and *VAM7* genes and analyze the function of their gene products in peroxisome degradation in *H. polymorpha.* The data of this study are contained in this paper.

2. Materials and methods

2.1. Micro-organisms and growth conditions

All *H. polymorpha* strains used are derivatives of NCYC495 [15] and are listed in Table 1. *H. polymorpha* strains were grown at 37 °C in (i) rich complex media (YPD) containing 1% yeast extract, 1% peptone and 1% glucose, (ii) mineral medium (MM) as described [16], supplemented with 0.25% ammonium sulphate using 0.5% glucose or 0.5% methanol as carbon source, and (iii) selective minimal medium containing 0.67% Yeast Nitrogen Base without amino acids (DIFCO) supplemented with 1% glucose (YND), 0.5% methanol (YNM), or 0.4% glucose together with 0.1 mM allyl alcohol (AA selection medium). For growth on plates, 1.5% granulated agar was added to the media. Whenever necessary, media were supplemented with 30 μg ml^{-1} leucine or 100 μg ml^{-1} zeocin.

For cloning purposes, *Escherichia coli* DH5α (Gibco-Brl, Gaithesburg, MD) was used and grown at 37 °C in LB (1% Bacto tryptone, 0.5% yeast extract, 0.5% NaCl), supplemented with zeocin (25 μg ml^{-1}), ampicillin (100 μg ml^{-1}) or kanamycin (50 μg ml^{-1}) when required.

Table 1
Hansenula polymorpha strains used in this study

Strain	Genotype and characteristics	Reference
NCYC495	*leu1.1* derivative	[15]
NCYC495	*leu1.1 ura3* derivative	[15]
HF246	NCYC495::(P_{AOX}*eGFP.SKL*)^{1c}; *leu1.1*	[23]
Pdd20-1	HF246::pREMI-Z; *leu1.1*; Pdd$^-$; zeo^R	This study
vam3-1	HF246 retransformed with the *VAM3* disruption cassette isolated from mutant Pdd20-1; *leu1.1*; Pdd$^-$; zeo^R	This study
eGFP.VAM3	NCYC495 transformed with pHIPX6-eGFP.PDD20	This study
vam7	NCYC495 *vam7*::*Hp-URA3*; *leu1.1*	This study
VAM7.eGFP	NCYC495 transformed with pHIPX6-VAM7.eGFP	This study
DsRED.SKL	NCYC495::(P_{AOX}*DsRED-T1.SKL*), *leu1.1*; zeo^R	[36]
DsRED.SKL/VAM7.eGFP	DsRED.SKL transformed with pHIPX6-VAM7-eGFP; zeo^R	This study

Abbreviation: zeo, zeocin.

2.2. Miscellaneous DNA techniques

Plasmids and oligonucleotide primers used in this study are listed in Tables 2 and 3, respectively. Standard DNA techniques were carried out essentially according to [17]. Electrotransformation of *H. polymorpha* was performed as described previously [18]. Yeast chromosomal DNA was isolated as described by Faber et al. [19]. DNA-modifying enzymes were used as recommended by the supplier (Roche, Almere, the Netherlands). For Southern- blot analysis the ECL direct nucleic-acid labeling and detection system was used (Amersham Corp., Arlington Heights, IL). DNA sequencing reactions were carried out at BaseClear (Leiden, The Netherlands) on a LiCor automated DNA-sequencer using dye primer chemistry (LiCor INC., Lincoln, NB). Oligonucleotide primers were obtained from Life Technologies (Breda, the Netherlands). For DNA sequence analysis, the Clone Manager 5 program (Scientific and Educational Software, Durham, USA) was used. BLAST algorithms [20] were used to screen databases at the National Center for Biotechnology Information (Bethesda, MD). The Clustal_Xprogram was used to align protein sequences [21], while the GeneDoc program (available at http://www.psc.edu/biomed/genedoc) was used to display the aligned sequences. The software TREECON for Windows [22] was used for the construction of phylogenetic trees.

2.3. Gene tagging mutagenesis and isolation of mutants

The RAndom Integration of Linear DNA Fragments (RALF) method [23] was used to generate yeast mutants. *H. polymorpha* HF246 was transformed with *Bam*HI-linearized pREMI-Z plasmid. Transformants were initially selected on YPD plates supplemented with zeocin, then screened using AA selection plates [24]. Allyl alcohol-sensitive colonies were subsequently screened for their peroxisome degradation-deficient (Pdd$^-$) phenotype using the AO activity plate assay as described by Titorenko et al. [25].

2.4. Identification of the gene disrupted in mutant Pdd20-1

To identify the gene disrupted by the pREMI-Z vector in mutant Pdd20-1, genomic DNA of mutant cells

Table 2
Plasmids used in this study

Plasmid	Relevant characteristics	Reference
pREMI-Z	Used for gene-tagging mutagenesis; zeo^R	[23]
pBSK-URA3	pBluescript SK$^+$ containing the 2.3 kb *H. polymorpha URA3* fragment, amp^R	[37]
pHIPX6	*E. coli*/*H. polymorpha* shuttle vector containing the *H. polymorpha PEX3* promoter, the *H. polymorpha AMO* terminator and the *S. cerevisiae LEU2* gene; kan^R	[38]
pHIPX6-eGFP.PDD20	pHIPX6 containing an *eGFP.VAM3* fusion gene; kan^R	This study
pHIPX6-VAM7.eGFP	pHIPX6 containing a *VAM7.eGFP* fusion gene; kan^R	This study
pFEM36	Plasmid containing the *GFP.SKL* gene; kan^R	[39]
pHS6A	*E. coli*/*H. polymorpha* shuttle vector derived from pBluescript II SK$^+$, amp^R, *S. cerevisiae LEU2* gene, HARS1	Lab. collection
pHS6A-VAM7	pHS6A with the entire *H. polymorpha VAM7* gene; amp^R	This study
pHIPX6-eGFP.ATG8	pHIPX6 containing an *eGFP.ATG8* fusion gene; kan^R	[36]

Abbreviations: amp, ampicillin; kan, kanamycin; zeo, zeocin.

Table 3
Primers used in this study

Name	Sequence
VAM7-del-F1	5′ GACTGGTGCGCGTCCCCCACGATCG 3′
VAM7-del-R1	5′ CATAATTGCGTTGCTGAACATCAGTTGAAGCTCCGTTCAAAAACTCCGCCAGCCC 3′
VAM7-del-F2	5′ GAAGAAGCGACGCCGATCCAGTTGATGTGCGGCTTGGACAATCAAGTCGACAGC 3′
VAM7-del-R2	5′ CCCGGAAATTCCACAATCCC 3′
VAM7-F3	5′ TGACCTCGCCATATTTCACG 3′
PDD20-1	5′ CACTGCTGTGAGAAGAAGAC 3′
PDD20-2	5′ ATCGTGTTTCATACTCTACG 3′
PDD20-S-GFP	5′ CTCGGCATGGACGAGCTGTACAAGATGTCGTTTGCCAACTTGGATC 3′
PDD20-AS	5′ GGGCACAGCCTCCTCTATTTAGTTC 3′
pHIPX6-F	5′ GCTCACAAGTGATACCCCATTCG 3′
FwVAM7	5′ TCAGGGATCCATGGTGGAGGTCAGAATACC 3′
RevVAM7GFP	5′ GGTGAACAGCTCCTCGCCCTTGCTCACGAGAATACGGCCAATTTTC 3′
RevGFP	5′ GGGCTACTTGTACAGCTCGTCCATGCCG 3′
pREMI-ori	5′ GATCTTTTCTACGGGGTCTG 3′
pREMI-tef	5′ CGGAGTCCGAGAAAATCTGG 3′

was isolated, digested with *Eco*RI, self-ligated and transformed into *E. coli*. After plasmid rescue, the flanking genomic regions were sequenced using the vector-based primers pREMI-ori and pREMI-tef [23]. Sequence analysis revealed that the pREMI-Z vector had integrated in the putative *H. polymorpha VAM3* gene (Fig. 1(a)). The nucleotide sequence of the *Hp-VAM3* gene was completed by sequencing an approximately 1-kb DNA fragment obtained by PCR with primers PDD20-1 and PDD20-2, using genomic DNA of wild-type *H. polymorpha* as template. The nucleotide sequence of *Hp-VAM3* was submitted to Genbank and assigned the accession number AY874422.

Sequence analysis of the genomic regions flanking pREMI-Z in the Pdd20-1 mutant indicated that 127 bp upstream of *Hp-VAM3* the startcodon of a putative homologue of the essential *S. cerevisiae POL1* gene, encoding a catalytic subunit of the DNA polymerase I complex, was located (Fig. 1(a)). Since this would place the promoter of the putative *Hp-POL1* gene partly inside the coding region of *Hp-VAM3*, this precluded construction of a null mutant lacking the entire *Hp-VAM3* ORF. Therefore, only the mutant disrupted by the pREMI-Z plasmid was used in our studies. To ensure that the mutant strain used carried only the disrupted *Hp-VAM3* gene, and no possible second site mutations, we isolated the RALF disruption cassette as a 3-kb fragment from the Pdd20-1 mutant by PCR, using primers PDD20-1 and PDD20-2 and transformed *H. polymorpha* HF246. Zeocin-resistant colonies were analysed by Southern blotting to identify the correct disruptant (data not shown). The resulting strain was designated *vam3-1*. AO activity plate assays demonstrated that both the Pdd20-1 and *vam3-1* mutants had the same weak Pdd$^-$ phenotype (data not shown).

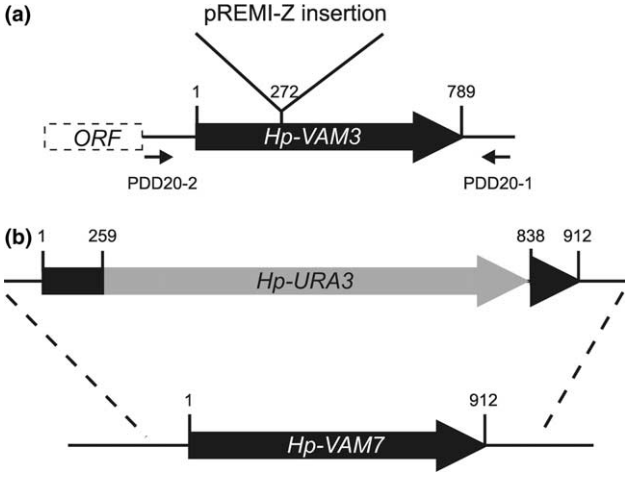

Fig. 1. (a) Schematic representation of the *H. polymorpha* chromosomal region that contains *VAM3*. The pREMI-Z integration site in the *vam3-1* mutant is shown. Also indicated is the start of a putative *Hp-POL1* gene upstream of the startcodon of *Hp-VAM3*. The location of the primers PDD20-1 and PDD20-2 is represented by arrows. The numbers refer to nucleotide numbers in the *VAM3*-coding sequence. (b) Schematic representation of the strategy to delete the *VAM7* gene from the *H. polymorpha* genome via double cross-over. The numbers refer to nucleotide numbers in the *VAM7*-coding sequence.

2.5. Construction of a H. polymorpha VAM7 null mutant

A TBLASTN search using the primary sequence of *S. cerevisiae* Vam7p as a query identified a single *Hp-VAM7* candidate gene in the *H. polymorpha* genome database [26]. The nucleotide sequence of *Hp-VAM7* has been submitted to Genbank and was assigned the accession number AY884835.

A strain deleted for *Hp-VAM7* (designated *vam7*) was constructed by replacing the region comprising nucleotides +260 to +837 by an auxotrophic marker (Fig. 1(b)). To this end, a *Hp-VAM7* deletion cassette was constructed by overlap PCR. First, two DNA fragments comprising the region −141 to +259 and + 838 to +1290 of the *Hp-VAM7* genomic region were obtained by PCR, using the primer combinations VAM7-del-F1 + VAM7-del-Rl and VAM7-del-F2 + VAM7-del-R2, respectively, and wild-type *H. polymorpha* DNA as template. Two of these primers, VAM7-del-Rl and VAM7-del-F2, contain DNA sequences that overlap with the *H. polymorpha URA3* promoter and terminator regions, respectively. In a second PCR step, the deletion cassette was synthesized using the products obtained after the first amplification reactions as primers and pBSK-URA3 as template. The resulting 2.4-kb fragment, which contains the *Hp-URA3* gene with flanking regions of the *VAM7* gene, was used to transform NCYC495 *leu1.1 ura3* cells. Proper deletion of *VAM7* was confirmed by Southern blotting (data not shown).

A plasmid containing the entire *Hp-VAM7* gene (region −707 to +1290) was isolated by PCR with the primers VAM7-F3 and VAM7-del-R2 using WT genomic *H. polymorpha* DNA as template. The resulting 2136-bp fragment was digested with *Xho*I and cloned between the *Sal*I and *Sma*I sites of the polylinker of vector pHS6A, resulting in plasmid pHS6A-VAM7.

2.6. Construction of strains synthesizing fluorescent versions of Hp-Vam3p and Hp-Vam7p

To obtain a *H. polymorpha* strain producing an eGFP.Vam3p fusion protein, we constructed plasmid pHIPX6-eGFP.PDD20 by overlap PCR as follows. Firstly, an 831-bp PCR fragment containing the entire *Hp-VAM3* coding region was obtained with primers PDD20-S-GFP and PDD20-AS using WT genomic *H. polymorpha* DNA as template. Primer PDD20-S-GFP contains DNA sequences that overlap with the 3′ end of the *eGFP* gene. The amplified fragment was purified and used in a second PCR with primer pHIPX6-F using plasmid pHIPX6-eGFP.ATG8 as template. The

obtained 1577 bp fragment, which contained *eGFP* fused in frame with *Hp-VAM3*, was digested with *Bam*HI and subsequently inserted in *Bam*HI + *Sma*I-digested pHIPX6. The resulting plasmid, pHIPX6-eGFP.PDD20, was transformed into *H. polymorpha* NCYC495 (*leu1.1*) cells to obtain strain eGFP.VAM3.

In a similar way, we constructed plasmid pHIPX6-VAM7.eGFP. First, a 946-bp PCR fragment containing the entire *Hp-VAM7* gene was obtained with primers FwVAM7 and RevVAM7GFP using WT genomic *H. polymorpha* DNA as template. Note that primer RevVAM7GFP contains DNA sequences that overlap with the 5′ end of the *eGFP* gene. The amplified fragment was used in a second PCR together with primer RevGFP and plasmid pFEM36 as template. The obtained 1639-bp fragment, which contained *Hp-VAM7* fused in frame with *eGFP*, was digested with *Bam*HI and subsequently inserted in *Bam*HI + *Sma*I-digested pHIPX6. The resulting plasmid, pHIPX6-VAM7.eGFP, was transformed into *H. polymorpha* NCYC495 (*leu1.1*) and DsRED.SKL cells to obtain strains VAM7.eGFP and DsRED.SKL/VAM7.eGFP, respectively.

2.7. Biochemical methods

Crude cell extracts were prepared as described [27]. Determination of protein concentrations, SDS–PAGE and Western blotting were performed by established procedures. The degradation of peroxisomes in batch-cultured cells of *H. polymorpha* was determined as described [25]. Induction of microautophagy by nitrogen limitation was performed as detailed in [4].

2.8. Morphological analysis

Intact cells were prepared for electron microscopy and immunocytochemistry as described previously [28]. Ultrathin unicryl sections were labelled using polyclonal antibodies raised in rabbits and goat-anti-rabbit antibodies conjugated to gold according to the instructions of the manufacturer (Amersham, Little Chalfont, UK). Fluorescence microscopy studies were performed using a Zeiss Axioskop microscope (Carl Zeiss, Göttingen, Germany). Vacuolar membranes were visualized using FM4-64 (final concentration of 2 μM) that was added to the cultures 30–45 min before analysis.

3. Results

3.1. Isolation of the H. polymorpha VAM3 and VAM7 genes

The *H. polymorpha VAM3* gene was identified within a collection of peroxisome degradation-defective (Pdd$^-$) mutants that had been isolated by gene tagging mutagenesis [23]. Of this collection, one mutant, designated Pdd20-1, had shown a reduced rate of peroxisome degradation relative to wild-type cells in AO activity plate assays [25]. Sequence analysis of the regions flanking the pREMI-Z vector in the genome of this mutant indicated that the vector had integrated at +272 in an ORF encoding a protein with similarity to the syntaxin family of t-SNARE molecules. Primary-sequence analyses and BLAST searches indicated that the protein was most similar to *S. cerevisiae* Vam3p and Pep12p and much less similar to other members of the syntaxin family. Recently the nucleotide sequence of the *H. polymorpha* genome has been determined [26]. Sequence analysis showed that the *H. polymorpha* genome encodes multiple SNAREs of the syntaxin family. Besides the isolated Pdd20p also a predicted protein can be identified (designated Hp-Pep12p; Genbank accession number AY884836), that is highly similar to *S. cerevisiae* Pep12p. An alignment of the primary sequences of these proteins is shown in Fig. 2(a). A phylogenetic tree showing the divergence between these sequences is depicted in Fig. 2(b). Analysis of these data indicates that the isolated protein clusters with *S. cerevisiae* Vam3p rather than Pep12p. From this we concluded that we had isolated the *H. polymorpha VAM3* gene. *Hp-VAM3* encodes a 262-amino-acid protein of approximately 30 kDa. Like other members of the syntaxin family, Hp-Vam3p contains a typical t-SNARE coiled-coil homology region (amino acids 170–232, see Fig. 2(a); see [29] and the references therein). Furthermore, similar to Sc-Vam3p, Hp-Vam3p contains a hydrophobic region at its extreme C-terminus (amino acids 244–260, see Fig. 2(a)) that presumably represents a transmembrane anchor (cf. [29]).

In *S. cerevisiae*, the t-SNARE Vam3p is involved in autophagy and the Cvt pathway [11]. As Vam3p functions in complex with Vam7p in baker's yeast [13,14], we decided to investigate the role of Vam7p in macropexophagy in *H. polymorpha* as well. We identified a putative *Hp-VAM7* gene in the *H. polymorpha* genome sequence ([26] Genbank AY884835) using the primary sequence of Sc-Vam7p as a query. *Hp-VAM7* encodes a protein of approximately 35 kDa with 39% identity to *S. cerevisiae* Vam7p (Fig. 2(c)). Primary-sequence analysis showed that like Sc-Vam7p, Hp-Vam7p contains a phox homology (PX) domain at its N-terminus (amino acids 1–124, Fig. 2(c)). For Sc-Vam7p, this domain has been demonstrated to bind to phosphatidylinositol-3-phosphate [30,31], and is required to recruit the protein to the vacuolar membrane. Furthermore, Hp-Vam7p contains coiled-coil regions of t-SNARE similarity (amino acids 232–302; Fig. 2(c)). Analysis of the hydropathy profile of the protein (not shown) indicated that, like Sc-Vam7p, the *Hp VAM7* gene product has no typical membrane-spanning regions.

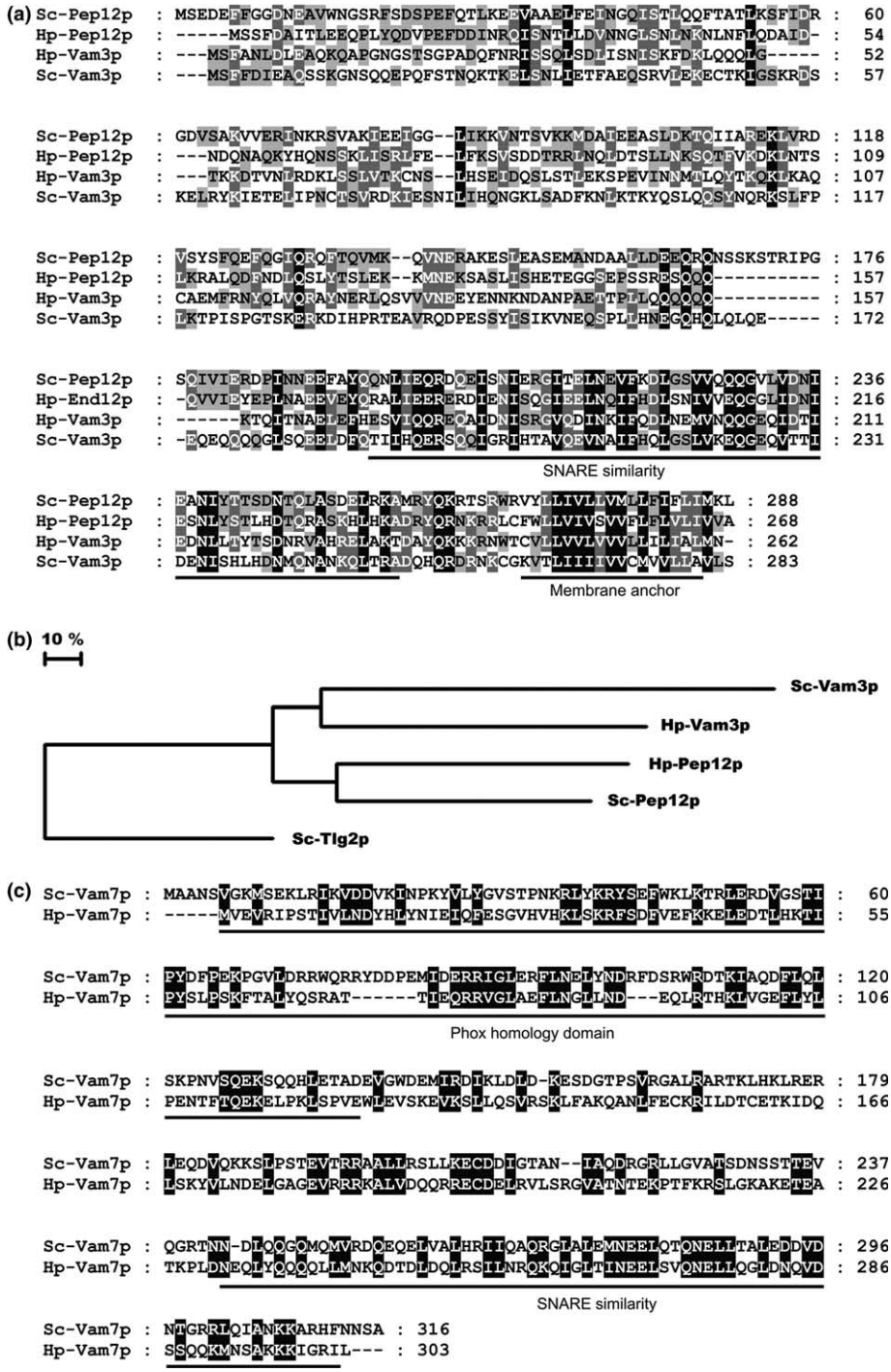

Fig. 2. (a) Alignment of the putative *H. polymorpha* Vam3p and closely related members of the syntaxin family of SNAREs identified in *H. polymorpha* and *S. cerevisiae*. The Hp-Vam3p primary sequence (Genbank accession number AY874422) was aligned with *S. cerevisiae* (Sc) Vam3p (Genbank AAC49737), Pep12p (SwissProt P32854), and the Pep12p homologue encoded by the *H. polymorpha* genome sequence ([26]; Genbank AY884836). The one-letter code is shown. The *bars* below the sequences indicate the t-SNARE similarity region and the C-terminal membrane anchor. Gaps were introduced to maximise the similarity. Residues that are similar in all proteins are in black; those that are similar in three of the proteins are shaded dark gray, while those that are similar in two of the proteins are shaded light gray. (b) Evolutionary tree of the putative *H. polymorpha* Vam3p (Genbank AY874422) and the most similar SNAREs of the syntaxin family identified in *H. polymorpha* (Hp-Pep12p, Genbank AY884836) and *S. cerevisiae* (Sc-Vam3p and Sc-Pep12p, Genbank AAC49737 and SwissProt P32854, respectively). As an outgroup, a member of the syntaxin family (Sc-Tlg2p, Swissprot Q08144) was chosen which has weaker similarity to Vam3p and Pep12p. The protein encoded by the isolated *PDD20* gene is more closely related to *S. cerevisiae* Vam3p than to *H. polymorpha* and *S. cerevisiae* Pep12p. (c) Alignment of the putative *H. polymorpha* Vam7p and *S. cerevisiae* Vam7p. The Hp-Vam7p primary sequence (Genbank AY884835) was aligned with *S. cerevisiae* (Sc) Vam7p (Genbank AAC49494). The one-letter code is shown. Gaps were introduced to maximise the similarity. Residues that are similar in both proteins are present in black boxes. The bars below the alignment indicate the N-terminal PX domain and the C-terminal region of t-SNARE similarity.

3.2. H. polymorpha vam7 *cells are impaired in macropexophagy and microautophagy*

Since plate assays provide only a qualitative indication of defects in peroxisome degradation, the *vam3-1* and *vam7* strains were analyzed in more detail after cultivation in liquid cultures. Growth experiments indicated that cells of both mutants had no defects in growth on glucose, glycerol or methanol (data not shown). However, in fluorescence microscopy studies using the vacuolar dye FM4-64, *vam7* cells appeared to contain highly fragmented vacuoles, while WT cells typically contain a single vacuole (Fig. 3). In the *vam3-1* mutant, often multiple vacuoles were present in the cells (Fig. 3; compare also Fig. 5(a)).

To analyse the fate of peroxisomes during macropexophagy, methanol-grown cells of both strains were exposed to glucose excess conditions. Under these conditions, in *vam3-1* cells the activity of the peroxisomal matrix protein alcohol oxidase (AO) declined, albeit somewhat slower than in WT cells (Fig. 4(a)). Also, analysis of AO protein levels by Western blotting demonstrated that selective peroxisome degradation was retarded in *vam3-1* cells (Fig. 4(b)). Electron-microscopical analysis – including inspection of $KMnO_4$-fixed cells (not shown) and immunocytochemistry, using α-AO antibodies – revealed that indeed peroxisomes were degraded via macropexophagy, since organelles became normally sequestered and were taken up by the vacuole (Fig. 5(a)).

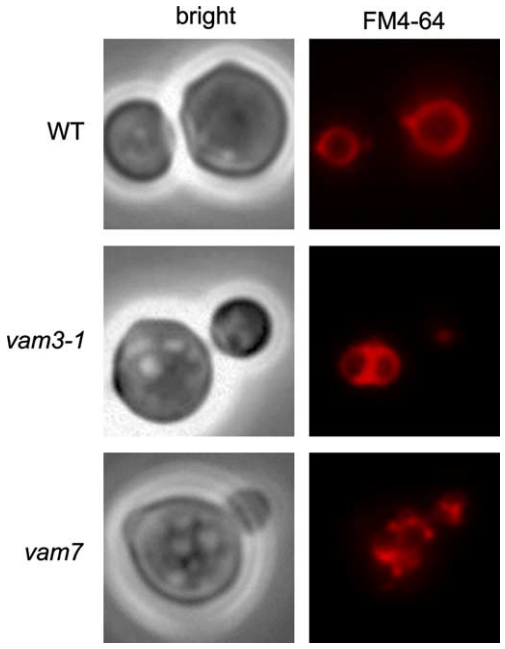

Fig. 3. *H. polymorpha vam3-1* and *vam7* cells contain multiple vacuoles. *H. polymorpha* WT, *vam3-1* and *vam7* cells were grown on methanol to the mid-exponential growth phase. Subsequently, FM4-64 was used to label vacuolar membranes, and the cells were inspected by fluorescence microscopy. In WT cells typically a single large vacuole is observed. In *vam3-1* cells often multiple vacuoles can be seen, while in *vam7* cells the vacuole appears to be fragmented into many small vesicular structures.

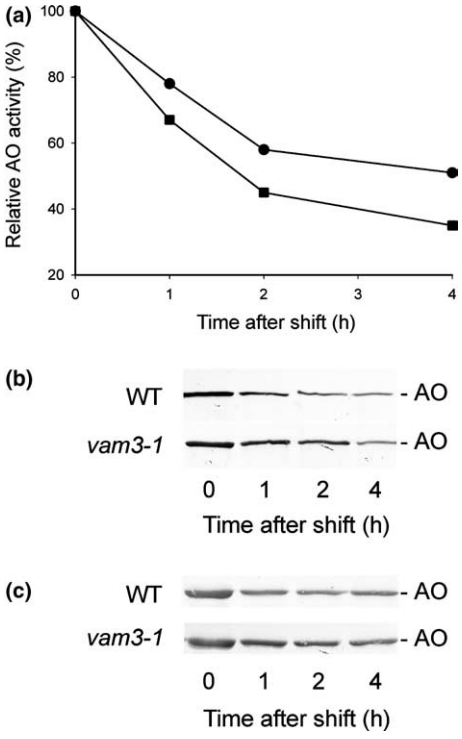

Fig. 4. *H. polymorpha vam3-1* cells are only weakly disturbed in macropexophagy and microautophagy. (a and b) Macropexophagy in *H. polymorpha* WT and *vam3-1* cells. Cells were grown on methanol-containing media to the mid-exponential growth phase, upon which glucose was added to the cultures to induce selective peroxisome degradation. (a) The enzyme activity of the peroxisomal marker protein AO was measured in crude extracts of *H. polymorpha* WT (squares) and *vam3-1* (circles) cells taken 0, 1, 2 and 4 h after the shift to the new environment. AO activities are expressed as percentage of the initial (methanol) value, which was set to 100%. Data are corrected for growth on glucose. (b) TCA samples of identically grown cells were taken and were prepared for Western blots. To correct for growth on glucose, equal volumes of culture were loaded per lane. The blots were decorated with antibodies against AO. (c) Western blots were prepared from cell extracts from methanol/ammonium sulphate-grown *H. polymorpha* wild-type (WT) and *vam3-1* cells shifted to methanol media lacking any nitrogen source to induce microautophagy. Samples were taken at the indicated time points. Equal amounts of protein were loaded per lane. Blots were decorated with polyclonal antibodies against AO protein. At both macropexophagy and microautophagy conditions the levels of AO activity and protein in WT cells decreased over time, indicating degradation of peroxisomes. AO degradation also occurred in *vam3-1* cells, albeit at a slower pace.

Identical experiments, performed on methanol-grown *vam7* cells adapted to glucose, showed that reduction in AO activity (not shown) and AO protein (Fig. 6(a)) did not occur. Electron-microscopical analysis demonstrated that peroxisomes remained intact during prolonged incubation of cells for four hours. Immunocytochemically, AO protein was never observed in the vacuolar lumen. However, initiation of peroxisome sequestration was not impaired in *vam7* cells,

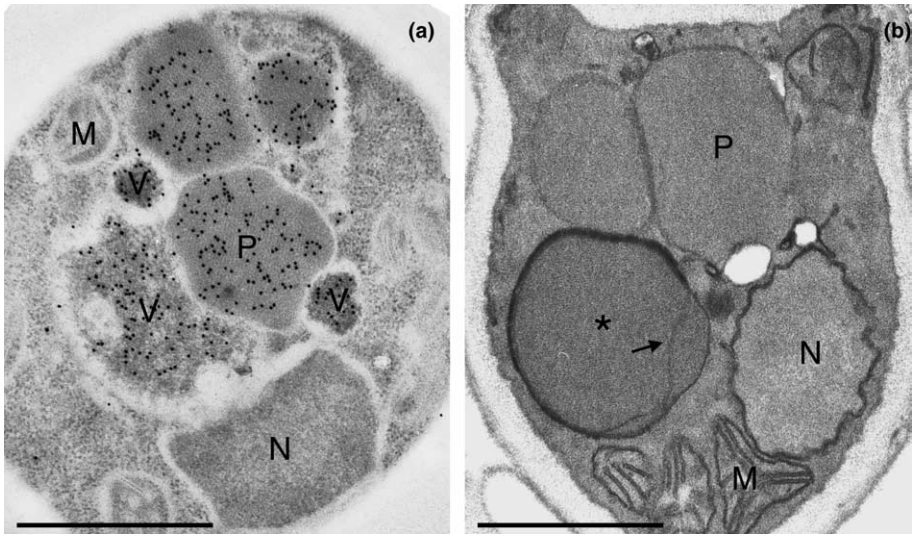

Fig. 5. Macropexophagy in *H. polymorpha vam3-1* and *vam7* cells. (a) Immunocytochemistry on ultrathin sections of methanol-grown *vam3-1* cells subjected to excess glucose for 1 h. The selective location of gold particles on both peroxisomal and vacuolar profiles after incubation with anti-AO antibodies shows that peroxisomes in *vam3-1* cells are being degraded. Note the presence of multiple vacuolar structures. (b) Peroxisomes in *vam7* cells become sequestered but are not taken up by the vacuole for degradation. Morphology of methanol-grown *vam7* cells that were exposed to glucose-excess conditions for 30 min. Cells were fixed with $KMnO_4$. Section of a cell showing the characteristic stretches of sequestering membrane that adhere to the peroxisomes, but fail to completely sequester the organelles. Note that the partially sequestered peroxisome (asterisk) appears to contain internal membranes (arrow). Key: M – mitochondrion, N – nucleus, P – peroxisome, V – vacuole. The bar represents 1 μm.

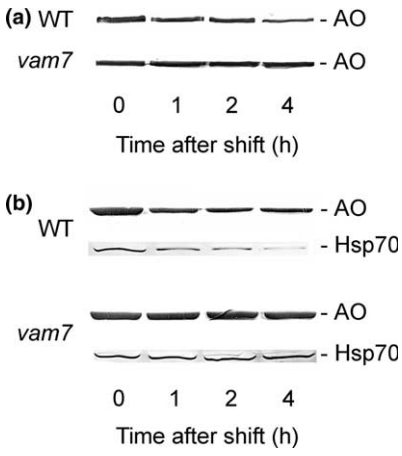

Fig. 6. *H. polymorpha vam7* cells are disturbed in macropexophagy and microautophagy. Western blots were prepared from cell extracts from methanol-grown *H. polymorpha* WT and *vam7* cells subjected to excess glucose conditions to induce macropexophagy (a) and from methanol/ammonium sulphate-grown *H. polymorpha* WT and *vam7* cells shifted to methanol media lacking any nitrogen source to induce microautophagy (b). Samples were taken at the indicated time points. In (a) equal volumes of cultures were loaded per lane to correct for the growth of the cells on glucose, while in (b) equal amounts of protein were loaded per lane. Blots were decorated with polyclonal antibodies against AO or Hsp70 protein. Upon induction of macropexophagy or microautophagy AO levels in *vam7* cells do not decrease over time, implying that peroxisomes are not degraded under these conditions, while in WT cells AO levels decrease significantly. Also, upon induction of microautophagy the levels of the cytosolic protein Hsp70 do not decrease, while a clear reduction in Hsp70 levels is observed in WT cells.

although sequestration has never been observed to be completed (Fig. 5(b)). These data are consistent with the view that completion of sequestration of peroxisomes and/or the fusion process between the sequestered organelle and the vacuolar membrane are affected in *vam7* cells, thus explaining the defect in macropexophagy.

We also analysed the fate of peroxisomes in *vam3-1* and *vam7* cells during microautophagy. To this purpose methanol-grown cells of both strains were shifted to methanol medium lacking any nitrogen source. Under these conditions, in *vam3-1* cells, AO protein levels decreased over time, suggesting that microautophagy is not blocked in this mutant, but only retarded as compared to WT cells (Fig. 4(c)). In contrast, in *vam7* cells AO protein levels remained unchanged, implying that peroxisomes were not degraded under these conditions (Fig. 6(b)). Moreover, in *vam7* cells, also the levels of the cytosolic marker protein Hsp70 remained unchanged, while in WT control cells Hsp70 levels decreased. Combined, these data suggest that *vam7* cells are fully blocked in both selective macropexophagy and non-selective microautophagy.

3.3. H. polymorpha vam7 *cells show aberrant peroxisome morphology*

In the macropexophagy experiments we observed that peroxisomes in methanol-grown *vam7* cells – and to a much lesser extent *vam3-1* cells (data not shown), but not WT cells – often showed aberrant morphologies in that the organelles appeared to have internal membrane

structures (compare Fig. 5(b)). The morphology of these peroxisomes varied from organelles that contained additional internal structures to organelles with double surrounding membranes and organelles that had internal vesicular-like inclusions. Immunocytochemistry using specific antisera against the major peroxisomal matrix proteins gave surprising results. Using α-catalase (CAT) and α-dihydroxyacetone synthase (DHAS) antisera, specific labeling was observed in all sub-peroxisomal compartments (Fig. 7(b) and (c)). However, using α-AO antibodies, labelling was confined to the larger sub-compartment of the organelle that probably represents an individually developed part of the organelle (Fig. 7(a)). To study this in more detail we analyzed by electron microscopy the kinetics of peroxisome induction in *vam7* cells after a shift of cells from glucose- to methanol-containing media. The data obtained indicate that during the initial hours of incubation of cells on methanol, peroxisome growth and development proceeded normally [cf. 32]. After approximately seven hours of incubation ($OD_{663} = 0.6$), the first aberrant structures were detected: developing peroxisomes were observed that were in intimate contact with various small vesicular membrane structures (Fig. 8(b)). Upon serial sectioning, such structures appeared to be extensions of mitochondria (Fig. 9). Relative to normal mitochondria, these structures showed increased electron densities. In addition, also membrane clusters were observed that were associated with the peroxisomes (Fig. 8(b) and (c)) and were also frequently detectable at mitochondria (Fig. 8(a)). Our data suggest that the small vesicular structures that are associated with the peroxisomal membrane are the initial sites of aberrant organelle formation and lead to the formation of additional peroxisomal membranes, which was observed after twelve hours of incubation ($OD_{663} = 1.5$) (cf. Fig. 9). After 16 h of incubation, when the cells entered the

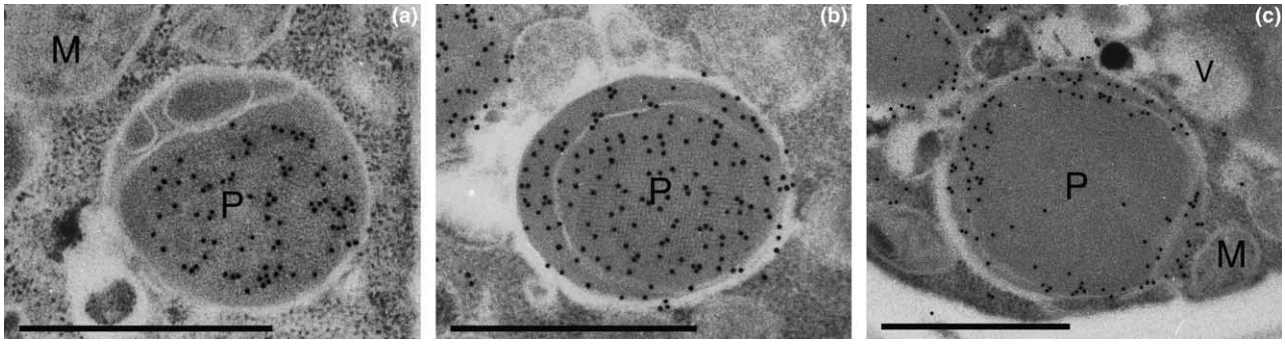

Fig. 7. The sub-compartments in peroxisomes of *H. polymorpha vam7* cells have a differential distribution of peroxisomal matrix proteins. Immunocytochemistry on ultrathin sections of *H. polymorpha vam7* cells grown on methanol for 16 h. Sections were labelled with specific antibodies against AO (a), DHAS (b) and CAT (c). The selective location of gold particles shows that AO protein is exclusively located in the larger sub-compartment of the peroxisome, while DHAS and CAT protein are present in all sub-compartments. Key: M – mitochondrion, P – peroxisome, V – vacuole. The bar represents 1 μm.

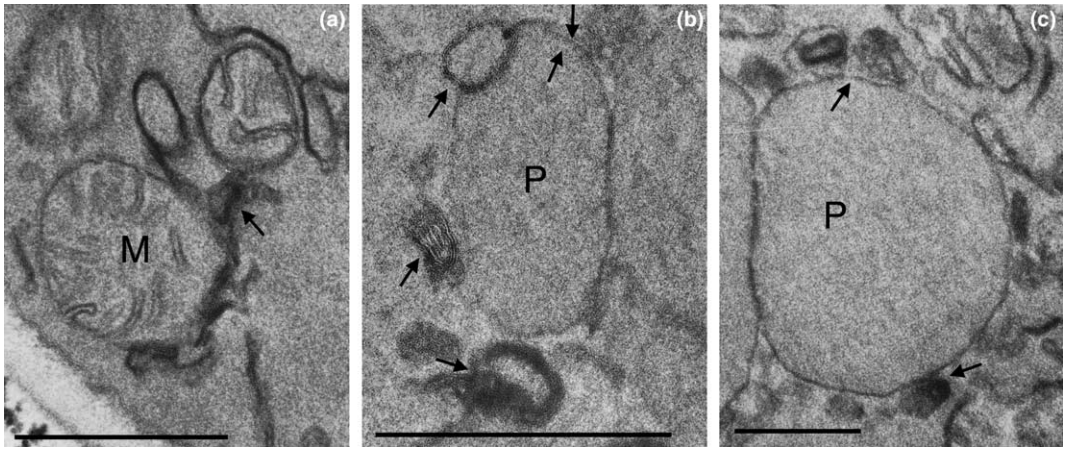

Fig. 8. Formation of peroxisomes with aberrant morphology in *vam7* cells. Morphology of *vam7* cells grown on methanol for 7 h (b) and 12 h (a and c). Cells were fixed with $KMnO_4$. (a) Section of a cell showing the characteristic clusters of additional membranes that are connected to mitochondria (arrow). (b) and (c) Show the initial stages in the formation of aberrant peroxisomes. Membrane clusters adhere to pre-existing peroxisomes, resulting in the formation of new peroxisomal compartments (arrows). Note the membrane clusters in the bottom part of b and c (arrows). Key: M – mitochondrion, P – peroxisome. The bar represents 0.5 μm.

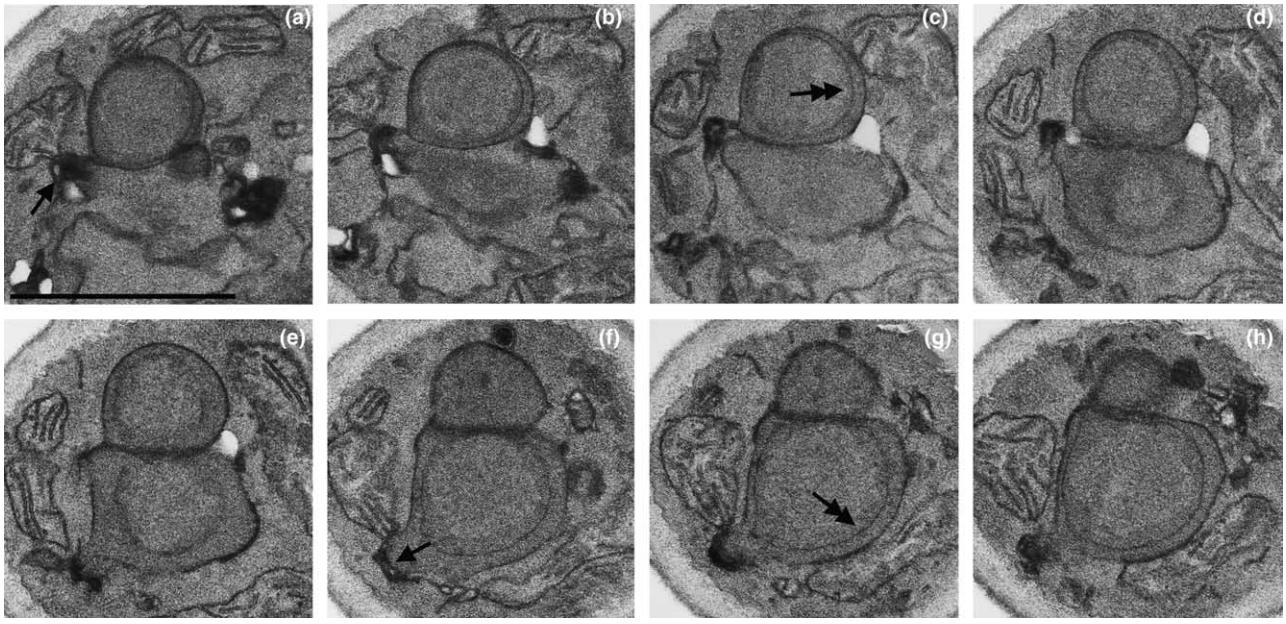

Fig. 9. The aberrant peroxisomes in *H. polymorpha vam7* cells are closely connected to mitochondria. Serial sections of methanol-grown *H. polymorpha vam7* cell fixed with $KMnO_4$. Two peroxisomes are shown both of which are closely connected to mitochondria via dense membrane structures (a, b, f and g, see arrows). In addition, both peroxisomes already have internal membranes (double arrows) that divide the organelles into multiple sub-compartments. The bar represents 1 μm.

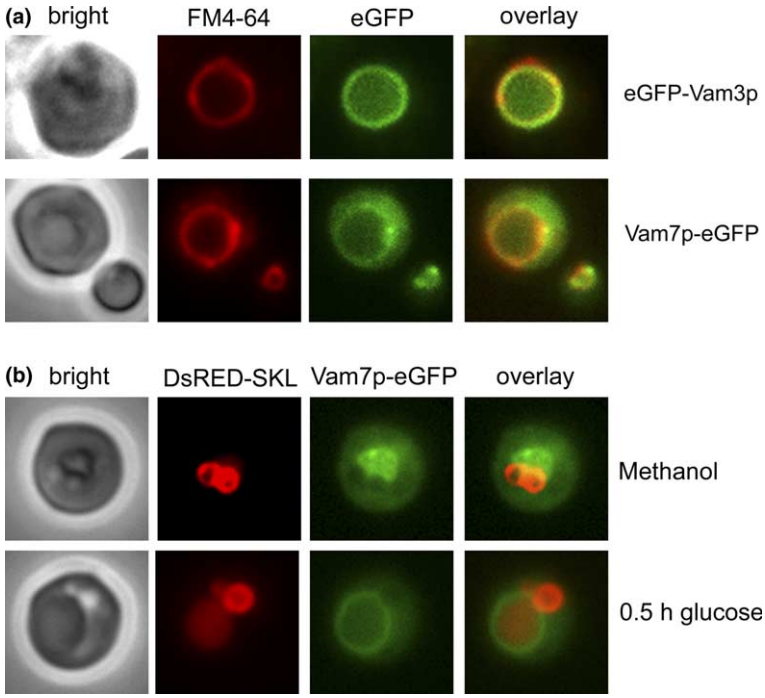

Fig. 10. (a) Localization of Vam3p and Vam7p in *H. polymorpha*. Methanol-grown *H. polymorpha* eGFP.VAM3 and VAM7.eGFP cells were incubated with FM4-64 to label the vacuolar membrane and were analysed by fluorescence microscopy. eGFP-Vam3p fluorescence co-localized exclusively with FM4-64 fluorescence, indicating that eGFP-Vam3p is located at the vacuolar membrane (a, top panels). In contrast, Vam7p-eGFP showed a dual localization, with a major portion of the protein co-localizing with the vacuolar membrane, while a significant amount of fluorescence was also observed in the cytosol (a, lower panels). (b) Vam7p-eGFP does not co-localize significantly with peroxisomes. Methanol-grown *H. polymorpha* DsRED.SKL/VAM7.eGFP cells were analysed by fluorescence microscopy. Red-fluorescent peroxisomes are located in close vicinity of the vacuole. However, concentration of Vam7p-eGFP fluorescence is not observed at the peroxisomal membrane (b, top panels). Upon induction of macropexophagy, red fluorescence is also observed inside the vacuole, indicating uptake and degradation of peroxisomes (b, lower panels).

late-exponential growth phase ($OD_{663} = 2.5$), organelles with an aberrant architecture were abundant (cf. Fig. 5(b) and Fig. 7).

3.4. Both Hp-Vam3p and Hp-Vam7p localize to the vacuole

To enable subcellular localization of Hp-Vam3p and Hp-Vam7p in *H. polymorpha*, we constructed plasmids allowing expression of *eGFP-VAM3* or *VAM7-eGFP* fusion genes under the control of the mild *H. polymorpha PEX3* promoter. In methanol-grown eGFP.VAM3 cells, the fusion protein exclusively localized to the vacuolar membrane as determined by the complete overlap of the eGFP fluorescence with that of the fluorescent vacuolar membrane marker FM4-64 (Fig. 10(a)). Similarly, also in VAM7.eGFP cells, eGFP fluorescence was mainly located at the vacuolar membrane in conjunction with significant fluorescence in the cytosol.

The peculiar peroxisomal profile observed in *vam7* cells prompted us to analyse a possible co-localization of a portion of Vam7p with peroxisomes. To this end we produced Vam7p.eGFP in WT *H. polymorpha* cells that also synthesize the fluorescent peroxisomal matrix protein DsRED.SKL. Analysis of methanol-grown cells of this strain showed that red-fluorescent peroxisomes were typically located in close vicinity of vacuoles (Fig. 10(b)). However, no other obvious co-localization of eGFP and DsRED.SKL fluorescence was observed. This suggest that Vam7p is probably not present in significant amounts on peroxisomes. As expected, upon a shift of methanol-grown DsRED.SKL/VAM7.eGFP cells to glucose-excess conditions, red fluorescence was observed also inside the vacuoles, indicating that the macropexophagy machinery was normally functional in this strain (Fig. 10(b)).

4. Discussion

We have isolated the *H. polymorpha* homologues of the *S. cerevisiae VAM3* and *VAM7* genes, encoding vacuolar t-SNAREs, and analyzed the properties of their gene products, Hp-Vam3p and Hp-Vam7p, respectively, in peroxisome homeostasis. This research was initiated by the isolation of the *H. polymorpha* Pdd20-1 mutant by gene-tagging mutagenesis that appeared to be disrupted in a gene encoding a member of the syntaxin family of t-SNAREs (cf. [33]). Our data indicate that the gene disrupted in Pdd20-1 in fact represents the *H. polymorpha VAM3* gene. Firstly, primary sequence analysis indicates that the protein encoded by the isolated gene is most related to Sc-Vam3p. Secondly, a Vam3p-eGFP fusion protein exclusively localized to the vacuolar membrane, as expected for this vacuolar t-SNARE [11,12]. Finally, the occurrence of multiple vacuoles in the *H. polymorpha vam3-1* mutant resembles the *S. cerevisiae vam3* mutant rather than the *pep12* mutant, which typically has single, large vacuoles [11].

Careful quantitative analysis revealed that deletion of Hp-Vam3p function had only a limited effect on macropexophagy and microautophagy. This was unexpected, in view of the essential role of this protein in membrane fusion processes in *S. cerevisiae* (i.e. autophagy, the Cvt pathway, vacuolar protein sorting and homotypic vacuole–vacuole fusion; [11–13]). By contrast, a second component of the *S. cerevisiae* vacuolar *cis*-SNARE complex to which Vam3p belongs, Vam7p, was essential for macropexophagy and microautophagy in *H. polymorpha*. We explain these data by assuming that another t-SNARE of the syntaxin family can (partly) take over the function of Hp-Vam3p in the vacuolar *cis*-SNARE complex. That this is not only a hypothetical possibility is evident from the finding that in *S. cerevisiae*, Pep12p-overproduction rescues all the phenotypes of a *vam3* mutant and vice versa, suggesting a clear redundancy in function [11]. A similar behaviour of Hp-Pep12p (or another member of the syntaxin family present in *H. polymorpha*) may very well explain the weak phenotype of the *vam3-1* mutant during peroxisome degradation. Also, the fact that aberrant peroxisomes were less frequently observed in the *vam3-1* mutant relative to the *vam7* mutant (see below) could be interpreted as being caused by suppression of a much stronger phenotype by another syntaxin-like protein. Finally, the isolated *H. polymorpha vam3-1* mutant does not appear to secrete the vacuolar proteinase carboxypeptidase Y to the extracellular medium (our unpublished data). By contrast, both *S. cerevisiae vam3* and *pep12* mutants are affected in CPY maturation [11,34]. Again, this points to functional redundancy of Hp-Vam3p. An alternative explanation for the observed weak Pdd^- phenotype of the *Hp-vam3* mutant is that the truncated gene might be still capable to produce a 90-amino-acid protein that could be partially functional. However, we feel that this explanation is less likely, because such a truncated version of Vam3p lacks both the region of t-SNARE similarity and the C-terminal membrane anchor, which have been demonstrated to be essential for its function in *S. cerevisiae* [35].

Deletion of *VAM7* affected both macropexophagy and microautophagy in *H. polymorpha*. In *S. cerevisiae*, Vam7p has been implicated in the transport of the Cvt cargo protein Ape1p to the vacuole [13]. Apart from a complete block in peroxisome degradation, deletion of *Hp-VAM7* also had an effect on peroxisome biogenesis. Surprisingly, peroxisomes with distinct sub-compartments were formed in methanol-grown *Hp-vam7* cells at later stages of growth on methanol. Their development was closely associated with electron-dense membrane material that seemed to originate from mitochondria.

There also appeared to be a bias in the distribution of peroxisomal matrix proteins over the separate compartments in the aberrant peroxisomes of *Hp-vam7* cells. In particular, the AO protein appeared not to be present in peroxisome sub-compartments formed during the later stages of exponential growth, in contrast, the DHAS and CAT proteins were localized in all sub-compartments. The reasons for these discrepancies in sub-peroxisomal location are unclear and require further investigation.

One possible explanation for the formation of these aberrant peroxisomes may be that, in the absence of Hp-Vam7p, the electron-dense membrane material does not become properly transported to or fused to the peroxisomal membrane. The implication of this interpretation would be that in wild-type cells a significant amount of membrane material that constitutes the peroxisome may actually originate from mitochondria. However, a clear co-localization of (a portion of) Vam7p-eGFP with peroxisomes, which would be expected in this scenario, could not be established (Fig. 10). Alternatively, the membrane flow may normally not be so significantly directed towards peroxisomes, but to other organelles, a process that has become blocked when Hp-Vam7p is absent, resulting in missorting of membrane material to peroxisomes. Clearly, these aspects require further analysis as well.

Acknowledgements

J.A.K.W.K is supported by a grant from Aard-en Levens Wetenschappen (ALW), which is subsidized by the Dutch Organization for the Advancement of Pure Research (NWO). I.J.K. holds a PIONIER grant from the Netherlands Organization for the Advancement of Pure Research (NWO/ALW). A.N.L.-H. was supported by a grant from CAPES-Brasilia/UERJ, Brazil. We gratefully acknowledge Rhein Biotech, Düsseldorf, Germany for generously providing the *H. polymorpha* genome sequence data. We thank Jurre Hageman, Marcel Lunenborg and Klaas Sjollema for expert assistance during various parts of this study.

References

[1] Bellu, A.R. and Kiel, J.A.K.W. (2003) Selective degradation of peroxisomes in yeasts. Microsc. Res. Tech. 61, 161–170.
[2] Farre, J.C. and Subramani, S. (2004) Peroxisome turnover by micropexophagy: an autophagy-related process. Trends Cell Biol. 14, 515–523.
[3] Noda, T. and Ohsumi, Y. (2004) Macroautophagy in yeast In: Autophagy (Klionsky, D.J., Ed.), pp. 70–83. Landes Biosciences, Georgetown, TX.
[4] Bellu, A.R., Kram, A.M., Kiel, J.A.K.W., Veenhuis, M. and van der Klei, I.J. (2001) Glucose-induced and nitrogen-starvation-induced peroxisome degradation are distinct processes in *Hansenula polymorpha* that involve both common and unique genes. FEMS Yeast Res. 1, 23–31.
[5] Onodera, J. and Ohsumi, Y. (2004) Ald6p is a preferred target for autophagy in yeast, *Saccharomyces cerevisiae*. J. Biol. Chem. 279, 16071–16076.
[6] Kiel, J.A.K.W., Komduur, J.A., van der Klei, I.J. and Veenhuis, M. (2003) Macropexophagy in *Hansenula polymorpha*: facts and views. FEBS Lett. 549, 1–6.
[7] Bellu, A.R., Komori, M., van der Klei, I.J., Kiel, J.A.K.W. and Veenhuis, M. (2001) Peroxisome biogenesis and selective degradation converge at Pex14p. J. Biol. Chem. 276, 44570–44574.
[8] Bellu, A.R., Salomons, F.A., Kiel, J.A.K.W., Veenhuis, M. and van der Klei, I.J. (2002) Removal of Pex3p is an important initial stage in selective peroxisome degradation in *Hansenula polymorpha*. J. Biol. Chem. 277, 42875–42880.
[9] Stromhaug, P.E. and Klionsky, D.J. (2004) Cytoplasm to vacuole targeting In: Autophagy (Klionsky, D.J., Ed.), pp. 84–106. Landes Biosciences, Georgetown, TX.
[10] Klionsky, D.J., Cregg, J.M., Dunn Jr., W.A., Emr, S.D., Sakai, Y., Sandoval, I.V., Sibirny, A., Subramani, S., Thumm, M., Veenhuis, M. and Ohsumi, Y. (2003) A unified nomenclature for yeast autophagy-related genes. Dev. Cell 5, 539–545.
[11] Darsow, T., Rieder, S.E. and Emr, S.D. (1997) A multispecificity syntaxin homologue, Vam3p, essential for autophagic and biosynthetic protein transport to the vacuole. J. Cell Biol. 138, 517–529.
[12] Wada, Y., Nakamura, N., Ohsumi, Y. and Hirata, A. (1997) Vam3p, a new member of syntaxin related protein, is required for vacuolar assembly in the yeast *Saccharomyces cerevisiae*. J. Cell Sci. 110, 1299–1306.
[13] Sato, T.K., Darsow, T. and Emr, S.D. (1998) Vam7p, a SNAP-25-like molecule, and Vam3p, a syntaxin homolog, function together in yeast vacuolar protein trafficking. Mol. Cell. Biol. 18, 5308–5319.
[14] Ungermann, C., von Mollard, G.F., Jensen, O.N., Margolis, N., Stevens, T.H. and Wickner, W. (1999) Three v-SNAREs and two t-SNAREs, present in a pentameric *cis*-SNARE complex on isolated vacuoles, are essential for homotypic fusion. J. Cell Biol. 145, 1435–1442.
[15] Gleeson, M.A.G. and Sudbery, P.E. (1988) Genetic analysis in the methylotrophic yeast *Hansenula polymorpha*. Yeast 4, 293–303.
[16] Van Dijken, J.P., Otto, R. and Harder, W. (1976) Growth of *Hansenula polymorpha* in a methanol-limited chemostat. Physiological responses due to the involvement of methanol oxidase as a key enzyme in methanol metabolism. Arch. Microbiol. 111, 137–144.
[17] Sambrook, J., Fritsch, E.F. and Maniatis, T. (1989) Molecular Cloning: A Laboratory Manual. Cold Sping Harbor Laboratory Press, Cold Spring Harbor, NY.
[18] Faber, K.N., Haima, P., Harder, W., Veenhuis, M. and AB, G. (1994) Highly-efficient electrotransformation of the yeast *Hansenula polymorpha*. Curr. Genet. 25, 305–310.
[19] Faber, K.N., Swaving, G.J., Faber, F., Ab, G., Harder, W., Veenhuis, M. and Haima, P. (1992) Chromosomal targeting of replicating plasmids in the yeast *Hansenula polymorpha*. J. Gen. Microbiol. 138, 2405–2416.
[20] Altschul, S.F., Madden, T.L., Schaffer, A.A., Zhang, J., Zhang, Z., Miller, W. and Lipman, D.J. (1997) Gapped BLAST and PSI-BLAST: a new generation of protein database search programs. Nucl. Acids Res. 25, 3389–3402.
[21] Thompson, J.D., Gibson, T.J., Plewniak, F., Jeanmougin, F. and Higgins, D.G. (1997) The CLUSTAL_X windows interface: flexible strategies for multiple sequence alignment aided by quality analysis tools. Nucl. Acids Res. 25, 4876–4882.
[22] Van de Peer, Y. and De Wachter, R. (1994) TREECON for Windows: a software package for the construction and drawing of

evolutionary trees for the Microsoft Windows environment. Comput. Appl. Biosci. 10, 569–570.
[23] Van Dijk, R., Faber, K.N., Hammond, A.T., Glick, B.S., Veenhuis, M. and Kiel, J.A.K.W. (2001) Tagging *Hansenula polymorpha* genes by random integration of linear DNA fragments. Mol. Genet. Genomics 266, 646–656.
[24] Komduur, J.A., Leão, A.N., Monastyrska, I., Veenhuis, M. and Kiel, J.A.K.W. (2002) Old yellow enzyme confers resistance of *Hansenula polymorpha* towards allyl alcohol. Curr. Genet. 41, 401–406.
[25] Titorenko, V.I., Keizer, I., Harder, W. and Veenhuis, M. (1995) Isolation and characterization of mutants impaired in the selective degradation of peroxisomes in the yeast *Hansenula polymorpha*. J. Bacteriol. 177, 357–363.
[26] Ramezani-Rad, M., Hollenberg, C.P., Lauber, J., Wedler, H., Griess, E., Wagner, C., Albermann, K., Hani, J., Piontek, M., Dahlems, U. and Gellissen, G. (2003) The *Hansenula polymorpha* (strain CBS4732) genome, sequencing and analysis. FEMS Yeast Res. 4, 207–215.
[27] Baerends, R.J.S., Faber, K.N., Kram, A.M., Kiel, J.A.K.W., van der Klei, I.J. and Veenhuis, M. (2000) A stretch of positively charged amino acids at the N terminus of *Hansenula polymorpha* Pex3p is involved in incorporation of the protein into the peroxisomal membrane. J. Biol. Chem. 275, 9986–9995.
[28] Waterham, H.R., Titorenko, V.I., Haima, P., Cregg, J.M., Harder, W. and Veenhuis, M. (1994) The *Hansenula polymorpha PER1* gene is essential for peroxisome biogenesis and encodes a peroxisomal matrix protein. J. Cell Biol. 127, 737–749.
[29] Laage, R. and Ungermann, C. (2001) The N-terminal domain of the t-SNARE Vam3p coordinates priming and docking in yeast vacuole fusion. Mol. Biol. Cell. 12, 3375–3385.
[30] Song, X., Xu, W., Zhang, A., Huang, G., Liang, X., Virbasius, J.V., Czech, M.P. and Zhou, G.W. (2001) Phox homology domains specifically bind phosphatidylinositol phosphates. Biochemistry 40, 8940–8944.
[31] Cheever, M.L., Sato, T.K., de Beer, T., Kutateladze, T.G., Emr, S.D. and Overduin, M. (2001) Phox domain interaction with PtdIns(3)P targets the Vam7 t-SNARE to vacuole membranes. Nat. Cell Biol. 3, 613–618.
[32] Veenhuis, M., Keizer, I. and Harder, W. (1979) Characterization of peroxisomes in glucose-grown *Hansenula polymorpha* and their development after the transfer of cells into methanol-containing media. Arch. Microbiol. 20, 167–175.
[33] Burri, L. and Lithgow, T. (2004) A complete set of SNAREs in yeast. Traffic 5, 45–52.
[34] Becherer, K.A., Rieder, S.E., Emr, S.D. and Jones, E.W. (1996) Novel syntaxin homologue, Pep12p, required for the sorting of lumenal hydrolases to the lysosome-like vacuole in yeast. Mol. Biol. Cell 7, 579–594.
[35] Wang, Y., Dulubova, I., Rizo, J. and Sudhof, T.C. (2001) Functional analysis of conserved structural elements in yeast syntaxin Vam3p. J. Biol. Chem. 276, 28598–28605.
[36] Monastyrska, I., van der Heide, M., Krikken, A.M., Kiel, J.A.K.W., van der Klei, I.J. and Veenhuis, M. (2005) Atg8 is essential for macropexophagy in *Hansenula polymorpha*. Traffic 6, 66–74.
[37] Leão-Helder, A.N., Krikken, A.M., van der Klei, I.J., Kiel, J.A.K.W. and Veenhuis, M. (2003) Transcriptional down-regulation of peroxisome numbers affects selective peroxisome degradation in *Hansenula polymorpha*. J. Biol. Chem. 278, 40749–40756.
[38] Kiel, J.A.K.W., Keizer-Gunnink, I.K., Krause, T., Komori, M. and Veenhuis, M. (1995) Heterologous complementation of peroxisome function in yeast: the *Saccharomyces cerevisiae PAS3* gene restores peroxisome biogenesis in a *Hansenula polymorpha per9* disruption mutant. FEBS Lett. 377, 434–438.
[39] Ozimek, P., Lahtchev, K., Kiel, J.A.K.W., Veenhuis, M. and van der Klei, I.J. (2004) *Hansenula polymorpha* Swi1p and Snf2p are essential for methanol utilisation. FEMS Yeast Res. 4, 673–682.